Dalton Transactions

Accepted Manuscript

ROYAL SOCIETY OF CHEMISTRY

www.rsc.org/dalton

Journal Name

ARTICLE

The Effect of Metal Ions on Photocatalytic Performance Based on Isostructural Framework

Received 00th January 20xx,
Accepted 00th January 20xx

DOI: 10.1039/x0xx00000x

www.rsc.org/

Zhichao Shao, Chao Huang, Xiao Han, Huarui wang, Angran Li, Yanbing Han, Kai Li*, Hongwei Hou* and Yaoting Fan

A series of 2D layered isostructural coordination complexes $\{[M_3(L)_2(H_2O)_6]\cdot H_2O\}_n$ (M = Mn (**1**), $Mn_{0.7}Co_{0.3}$ (**2**), $Mn_{0.5}Co_{0.5}$ (**3**), $Mn_{0.3}Co_{0.7}$ (**4**), and Co (**5**), respectively, H_3L=1-aminobenzene-3,4,5-tricarboxylic acid) have been synthesized under hydrothermal conditions, and applied to catalyze the reaction of degenerating organic dyes under visible light irradiation. The photocatalytic results indicate that complex **5** exhibits good photocatalytic properties in the presence of H_2O_2, while **1** can restrain the photodegradation of organic dyes. Remarkably, when Mn ions are gradually replaced by Co ions in complexes, photocatalytic activities of **1**-**5** turn from inhibition to promotion, which is a controllable regulation of photocatalytic properties via changing metal ions. Moreover, by using novel magnetic analysis methods and diffuse-reflectance UV/Vis spectra analysis methods, we explain the influence of center metal ions on the photocatalytic performance.

Introduction

At present, humanity is faced with serious environmental problems related to water pollutions.[1] Considerable efforts have been made in treating wastewater with many methods such as adsorption and separation,[2] chemical treatment,[3] and photocatalysis,[4] et. al. In these methods, photocatalysis under visible light irradiation is a convenient and recyclable approach for degrading organic dyes without further contamination.[5] Compared with traditional photocatalyst (such as TiO_2, metal titanate and niobate, *et. al*), coordination polymers (CPs) material not only can offer large interfacial surface areas and multiple routes for band gap engineering through compositional and structural control,[6] but also can be recovered from the solvent for reuse conveniently. The application of CPs driven by visible-light photocatalysis dye degradation has been reported recently,[7] and CPs with narrow band gaps may have broad prospects in developing efficient photocatalytic materials.[8]

According to the reports about CPs photocatalytic degradation of dyes, the factors affecting photocatalytic effect are concentrated on the structure of complexes[9,10] and size of dye molecules.[11] However, the chemical environment of center metals as an important factor influencing photocatalytic behaviors has not been studied and discussed. In the light of approved photocatalytic mechanism based on the electronic excitation and transformation,[12] since different center metal ions in CPs have a variety of electronic configurations, we suspect which would produce great impacts on the photocatalytic properties. To systematically gain insight into the above relationship, the isomorphous coordination complexes and intermediate M-M' coordination complexes should be introduced. Because of excluding the effect of ligands and geometries, the research of isostructural CPs is beneficial to find out the relationship between metal ions and the corresponding influence on the photocatalytic behaviors.

In this work, we use 1-aminobenzene-3,4,5-tricarboxylic acid (H_3L) as the ligand to obtain a series of isomorphous coordination complexes $\{[M_3(L)_2(H_2O)_6]\cdot H_2O\}_n$ (M=Mn (**1**), $Mn_{0.7}Co_{0.3}$ (**2**), $Mn_{0.5}Co_{0.5}$ (**3**), $Mn_{0.3}Co_{0.7}$ (**4**), and Co (**5**), respectively). Complex **5** exhibits preeminent photocatalysis activities on the degradation of organic dyes (Gentian violet, Methyl orange, Methylene blue, Rhodamine B, Rhodamine 6G and Fluorescein) under visible light irradiation, while **1** can restrain the photodegradation of dyes. When the ratios of Co ions increase gradually in complexes, photocatalytic activities of **1**-**5** turn from inhibition to promotion, which can offer a controllable regulation of photocatalytic properties by changing metal ions. In order to investigate the chemical environment of center metals, a novel magnetic analysis method was introduced to detect single electron coupling in the photocatalysts. As combining the magnetic analysis method with the diffuse-reflectance UV/Vis spectra analysis method, the internal causes of center metal ions modulating the photocatalytic properties have been explained.

Experimental

Materials and physical measurements

All the solvents and reagents were purchased from commercial source without further purification. The data of elemental analyses (C, N and H) were collected by a FLASH EA 1112 elemental analyzer.. Thermogravimetric analyses (TGA) were performed on a

The College of Chemistry and Molecular Engineering, Zhengzhou University, Zhengzhou, Henan, 450001, P. R. China

Electronic Supplementary Information (ESI) available: Crystallographic parameters, structure figures,PXRD, TGA, MS spectrum, UV/Vis spectra. CCDC 1058222-1058223. For ESI and crystallographic data in CIF See DOI: 10.1039/x0xx00000x

Netzsch STA 449C thermal analyzer at a heating rate of 10 °C min^{-1} in air. The Fourier Transform Infra-Red (FT-IR) spectra were carried out on a Bruker Tensor 27 spectrophotometer in the range of 400-4000 cm^{-1}. Atomic absorption spectrometer analysis (AAS) were tested on a Hitachi Z-8000 spectrometer. Mass spectra (MS) were obtained on Agilent Technologies 6420 Triple QuadLC/MS without the LC part. Variable-temperature magnetic susceptibilities were measured by a MPMS-7 SQUID magnetometer. Diamagnetic corrections were performed with Pascal's constants. Powder X-ray Diffraction (PXRD) patterns were obtained by Cu $K\alpha_1$ radiation on a PANalytical X'Pert PRO diffractometer.

Preparation of complexes

$\{[Mn_3(L)_2(H_2O)_6]\cdot H_2O\}_n$ (**1**) A mixture of $Mn(CH_3COO)_2\cdot 4H_2O$ (0.025 g, 0.1 mmol), 1-aminobenzene-3,4,5-tricarboxylic acid (H_3L) (0.022 g, 0.1 mmol), ethanol (2 mL), and H_2O (6 mL) was stirred and adjusted to pH 9 with 2 M NaOH solution, then sealed in a 15 mL Teflon-lined stainless autoclave at 120 °C for 1 day, followed by slow cooling to room temperature. murrey crystals of **1** were obtained in a yield of 48% based on H_3L. Anal. Calcd (%) for $C_{18}H_{24}Mn_3N_2O_{20}$, C, 28.68; H, 3.18; N, 3.71. Found: C, 28.67; H, 3.22; N, 3.52. IR (KBr, cm^{-1}): 3597m, 3421s, 1625m, 1588m, 1439m, 1371s, 1343s, 1111w, 808w, 732w, 632w.

$\{[M_3(L)_2(H_2O)_6]\cdot H_2O\}_n$ (**2**-**4**) A procedure similar to **1** was employed to synthesize heterometallic CPs **2**-**4** except that the manganese source was replaced by a mixture of $Co(CH_3COO)_2$ and $Mn(CH_3COO)_2$ with a ratio of 3:7, 5:5 and 7:3, respectively. Crystal color becomes shallow gradually. The relative molar ratio of Mn to Co determined by AAS for **2** ($\{[Mn_{2.1}Co_{0.9}(L)_2\cdot(H_2O)_6]\cdot H_2O\}_n$), **3** ($\{[Mn_{1.5}Co_{1.5}(L)_2\cdot(H_2O)_6]\cdot H_2O\}_n$) and **4** ($\{[Mn_{0.9}Co_{2.1}(L)_2\cdot(H_2O)_6]\cdot H_2O\}_n$).

$\{[Co_3(L)_2(H_2O)_6]\cdot H_2O\}_n$ (**5**) A mixture of $Co(CH_3COO)_2\cdot 4H_2O$ (0.025 g, 0.1 mmol), 1-aminobenzene-3,4,5-tricarboxylic acid (H_3L) (0.022 g, 0.1 mmol), ethanol (2 mL), and H_2O (8 mL) was stirred and adjusted to pH 9 with 2 M NaOH solution, then sealed in a 15 mL Teflon-lined stainless autoclave at 120 °C for 2 days, and followed by slow cooling to room temperature at a rate of 5 °C/h. Purple block crystals of **5** were obtained in a yield of 79% based on H_3L. Anal. Calcd (%) for $C_{18}H_{24}Co_3N_2O_{20}$, C, 28.23; H, 3.14; N, 3.66. Found: C, 27.46; H, 3.37; N, 3.32. IR (KBr, cm^{-1}): 3600m, 3372s, 1623m, 1421m, 1373s, 1348s, 1039w, 819w, 724w, 630w.

Single crystal X-ray crystallography

The crystallographic data of **1**-**5** were collected on a Rigaku Saturn 724 CCD diffractomer with Mo Kα radiation (λ = 0.71073 Å). The data were corrected by Lorentz and polarization effects. Absorption corrections were applied by utilizing numerical program. The structures were solved by direct methods and refined with a full-matrix least-squares technique based on F^2 with the SHELXL-97 crystallographic software package.[13] Hydrogen atoms were placed at calculated positions and refined as riding atoms with isotropic displacement parameters. Crystallographic data and structure processing parameters for **1** and **5** are summarized in Table 1. Selected bond lengths and bond angles of **1** and **5** are listed in Table S1. Crystallographic parameters of **2**-**4** are showed in Table S2.

Photocatalytic measurement

Photocatalytic experiments were carried out in aqueous solution. 20 mg sample of the complexes **1**-**5** and 30% H_2O_2 (0.05 mL) were added into 6 mL dyes (2×10^{-5} mol/L) aqueous solution. The mixture was stirred for an hour in dark environment to get a balance between adsorption and desorption. Then, the solution was stirred constantly upon the irradiation of Xe lamp (500 W). 0.5 mL sample from the reaction system was taken every 12 min, and the supernatant liquid was obtained by centrifugation for the UV/Vis analysis.

Table 1 Crystallographic data and structure refinement details for complexes **1** and **5**

Compound	**1**	**5**
formula	$C_{18}H_{24}Mn_3N_2O_{20}$	$C_{18}H_{24}Co_3N_2O_{20}$
F_w	753.21	765.18
T/K	293(2)	293(2)
l (Mo–Ka)/Å	0.71073	0.71073
Crystsyst	*Triclinic*	*Triclinic*
Space group	*P*-1	*P*-1
a/Å	7.4253(15)	7.4098(15)
b/Å	8.5276(17)	8.4255(17)
c/Å	10.395(2)	10.209(2)
α (deg)	82.75(3)	82.46(3)
β (deg)	83.46(3)	83.41(3)
γ (deg)	79.86(3)	79.14(3)
V ($Å^3$)	639.9(2)	617.9(2)
Z	1	1
D_{calcd}(g cm^{-3})	1.955	2.056
F(000)	381	387
μ (mm^{-1})	25.50	25.50
GOF	1.089	1.083
R_1 ($I > 2\sigma(I)$)	0.0351	0.0354
wR_2 ($I > 2\sigma(I)$)	0.0825	0.0877

$R = [\sum || F_0| - |F_d|| / \sum |F_0|]$, $R_W = \sum_W [|F_0^2 - Fc^2|^2 / \sum_W (|F_w|^2)^2]^{1/2}$

Results and discussion

Crystal structures

Single-crystal X-ray diffraction analysis reveals that complexes **1**-**5** are isostructural (Fig. S1), thus only **5** is discussed herein in detail. Complex **5** crystallizes in triclinic space group *P*-1. As shown in Fig. 1a, the asymmetric unit contains one and a half Co^{2+}, one L^{3-}, three coordinated H_2O molecules. Co1 ions are six coordinated and display distorted octahedral coordination geometry, surrounded by four O atoms (O4, O4a, O6 and O6c) from L^{3-}, and two O atoms (O5 and O5a) from two H_2O molecules. For Co2, the coordination environment also is a distorted octahedron with the equatorial plane occupied by three O atoms (O1, O6, and O9) and one N1 atom. One O8 atom and one O2 atom in the axial sites. The Co-O bond lengths fall in the range of 2.055(7)-2.165(7) Å, similar to the values found in other cobalt complexes.[14] The length of Co(2)-N(1) is 2.174(7) Å.

The L^{3-} in **5** is completely deprotonated, along with three carboxylic groups acting as μ^1-η^1:η^0, μ^1-η^2:η^0, and μ^2-η^1:η^1 modes in a clockwise direction, respectively. On the basis of these connection modes, Co2, and symmetry-related Co2a atom are linked together by two carboxylate groups in μ^1-η^2:η^0 and μ^1-η^2:η^0 to give a binuclear $[Co_2(CO_2)_2]$ unit, the binuclear units and Co1 are connected commutatively by μ^1-η^2:η^0 carboxylate bridges, which assembled into a 1D chain. The 1D chains are interconnected in a parallel manner and united each other via the Co-N connections to

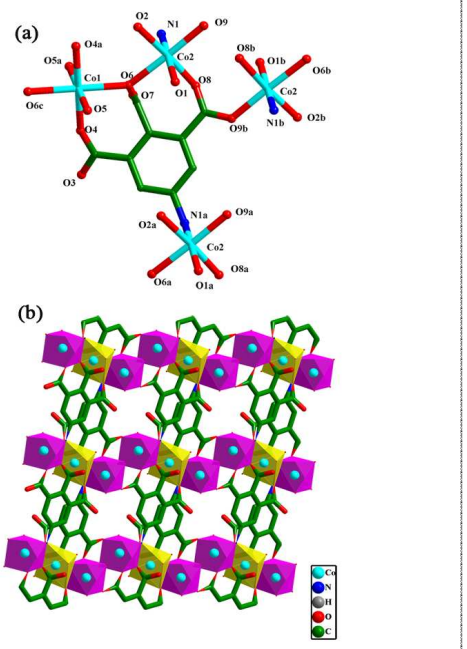

Fig. 1 (a) Coordination environment around Co^{II}. (b) View of 2D network of **5**.

afford a 2D layer net (Fig. S1b). In addition, strong hydrogen bond (O2···O3=2.701 Å, symmetry codes: x-1, y, z in Table S3) interactions contribute to the formation of a 3D supramolecular framework (Fig. S1c).

In order to understand the structure more intuitively, the connection method of compelx **5** was further analysed. For the overall 2D sheet formed, if just the coordination links are taken into account, a special metal chain are appeared by connecting alternately between the binuclear $[Co_2(CO_2)_2]$ unit and Co1, The metal chains are interconnected in a parallel manner and united each other via the L^{3-}. However, we found that hydrogen bonds played an important role in the formation of 3D supramolecular framework. If the strong hydrogen bonding is also considered, the ligands become 4-connecting nodes, Co1 are 2-connecting nodes and the $[Co_2(CO_2)_2]$-(H_2O) act as the 6-connected nodes. Then the structure of **5** turns into a very complicated 3D (2,4,6)-connected network, [15] Accordingly, the overall Schläfli symbol becomes $\{4^3.8^3\}_2\{4^6.6^6.8^3\}\{8\}$ (Fig. 2).

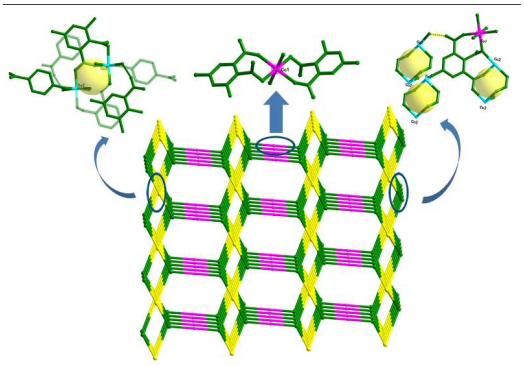

Fig. 2 A schematic diagram of the 3D (2,4,6)-connected trinodal network with $\{4^3.8^3\}_2\{4^6.6^6.8^3\}\{8\}$ topology of **5,** the ligands become 4-connecting nodes, Co1 are 2-connecting nodes, and the $[Co_2(CO_2)_2]$-(H_2O) act as 6-connecting nodes by the hydrogen-bonded links (O2···O3=2.701 Å, symmetry codes: x-1, y, z).

Thermal properties and PXRD

The purity of complexes **1** and **5** was performed by comparison of experimental PXRD patterns with the simulated pattern which were derived from the X-ray single crystal data (Fig. S2). Since CPs are potential function materials, the thermal stability is an important measure to verify the application value. Herein, TGA of complexes **1** and **5** were performed as shown in Fig. S3. For **1**, the first mass loss of 16.9% from 121 to 209 °C could be attributed to the release of one guest H_2O molecule and six coordination water molecules (calcd 16.8%). The overall framework of **1** begins to collapse from 327 °C, corresponding to the decomposition of L^{3-}. The remaining weight is in accordance with the formation of MnO. For **5**, the complex shows a mass loss of 16.6% from 70 to 244 °C, which may also be due to the release of H_2O molecules (calcd 16.4%). The overall framework of **5** begins to collapse from 310 °C. The final remaining residue of 31.9% is corresponding to the formation of CoO.

Photocatalysis property

Most of the photocatalytic reactions take place in the heterogeneous system. For recycling purpose, photocatalyst should be compatible with multi-solvents. Due to dyestuff pollution tend to occur in the water, verifing the stability of the catalyst in water solution is necessary, solvent resistance properties of **1**-**5** in water system were studied primarily by suspending samples in boiling water for 48 h. During this process, the samples were observed under an optical microscope periodically. After that, the unit-cell parameters were measured by single-crystal X-ray diffraction and the integrity of the frameworks were checked out by comparison of experimental PXRD patterns with the simulated pattern which were

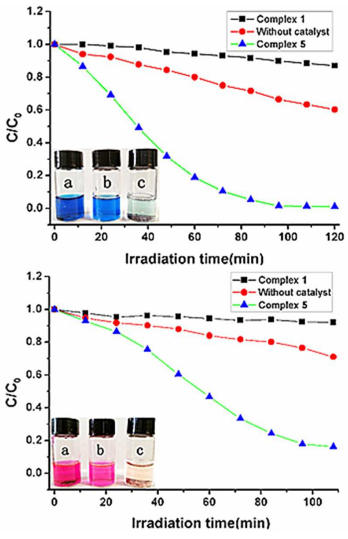

Fig. 3 Photocatalytic decomposition of MB solution (up) and RhB solution (down) in the presence of complexes **1**, **5** and the control experiment without any catalyst under the same conditions (a: **1**, b: without catalyst, c: **5**).

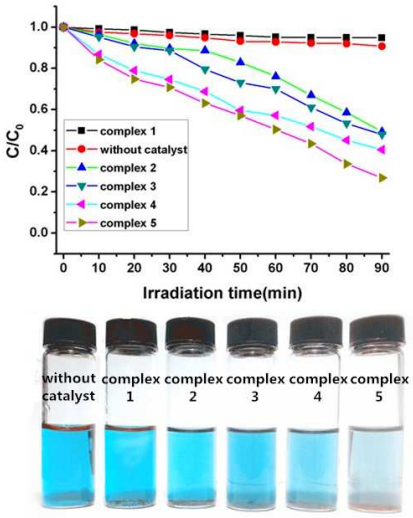

Fig. 4 Photocatalytic decomposition of MB solution in the presence of complexes **1**-**5** after irradiation for 90 min.

derived from the X-ray single crystal data (Fig. S4). As a result, the crystal appearance were almost unchanged and primary frameworks were intact throughout the process. The outstanding chemical resistance of the five complexes in refluxing water may be attributed to the following reasons: (i) the small bridging ligand, (ii) the short distance between chains, (iii) the existence of strong hydrogen bond between layers. In addition, crystal structure analysis suggests that there are two coordinated water molecules per metal ion site, which are good leaving groups and will be beneficial to make accessible substrates with the catalytic active sites in the reaction process. Thus, complexes **1**-**5** are likely to be excellent candidates as photocatalysts.

To explore the efficacies of photocatalytic behavior of **1** and **5**, the photocatalytic decomposition of organic dyes were investigated. Remarkablely, complex **5** exhibits good photocatalytic properties in the presence of H_2O_2. However, **1** can restrain the photodegradation of dyes. Analogous photocatalytic phenomenon are observed in six kinds of dyes (Gentian violet, Methyl orange, Methylene blue (MB), Rhodamine B (RhB), Rhod amine 6G and Fluorescein) (Fig. S5). Thus , only MB and RhB are discussed herein in detail, and the changes in the C_t/C_0 plot of MB/RhB solutions versus irradiation time are showed in Fig. 3 (wherein C_0 and C_t is the initial concentration and the concentration after irradiation for a few minutes). The characteristic absorption at 654 nm was selected to monitor photocatalytic degradation process of MB. The degradation ration reaches to 98.9% for complex **5**, 39.79% for control experiments and only 13.01% for complex **1** after 2 h of irradiation. Similar procedures were performed to inspect the photocatalytic activities at 554 nm for degradation of RhB. The calculation results show that it is 83.4% for complex **5**, 20.08% for control experiments and 13.01% for complex **1**. The increased photocatalytic decomposition rate indicates that complex **5** is vigorous for the decomposition of MB/RhB under visible light, while complex **1** can restrain the photodegradation of dyes. This phenomenon is also verified in experiments for other dyes.

In order to investigate the influence of metal ions on photocatalytic performance, isostructural coordination complexes **2**-**4** are applied degradation experiment. A notable photocatalytic phenomenon are observed. When the Mn ions are gradually replaced by Co ions, the photocatalytic abilities enhance regularly. These results indicated that change of center metals can affect the catalytic property to a promoting catalysis in decomposing organic dyes (Fig. 4).

Experiment results reveal that complex **5** can be a potential candidate as photocatalyst in decomposing most organic pollutants (Fig. S6). The results of MS show that dye molecules have been decomposed completely (Fig. S7). Clearly, with the size of dyes molecular increasing, the degradation rate reduces gradually (Fig. S8), the reason may be that space steric hindrance of large molecular volume. It is notable that the stability of **5** as a visible light photocatalyst is excellent. After repeating the photocatalytic degradation of MB for three times, similar photocatalytic efficiency were emerged (Fig. 5). The PXRD patterns after repeated bleaching experiment are almost the same as that of the as-prepared sample (Fig. S9).

Influence of metal ions on photocatalytic

With the development of CPs materials, the application of CPs as novel photocatalyst on dye degradation were reported recently.[7-10] The correlative mechanism has been also researched and verified. According to the reported photocatalytic mechanism, the activation effects of CPs in the photocatalytic degradation were attributed to the presence of hydroxyl radicals (·OH), which could degrade the organic dyes effectively. Hydroxyl radicals were generated by two possible routes during the whole photocatalytic process: (i) electrons (e^-) in valence bond (VB) could be excited to conduction band (CB) with the energy of visible light. The electrons with highly active state would transfer to oxygen radicals ($\cdot O_2^-$) to produce hydroxyl radicals. At the same time, the interaction between hydroxyl (OH^-) adsorbed on the CPs interaction and the hole (h^+) retained in the VB can also generate hydroxyl radicals.[16] (ii) Metal ions in CPs could react with H_2O_2 to generate hydroxyl radicals through a Fenton-like reaction.[17] The mechanism mentioned above have an universal adaptability, which can also be applied to our system.

In our catalytic system, the change of center metal ions is the most important factor. Therefore, a further discussion on the effect of photocatalytic performance with different metal ions was carried. For the purpose of investigating the chemical environment of center metals, magnetic behaviours and UV/Vis absorption spectrum of **1** and **5** are measured, respectively. As functional carriers, the different SBUs may be responsible for the discrepancy in photocatalytic activities owing to their diverse single electron

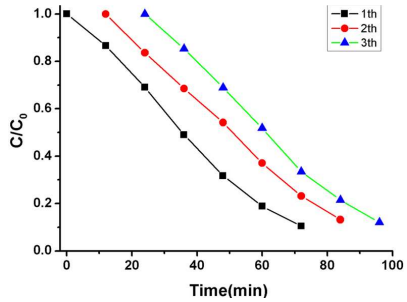

Fig. 5 Recycling test on **5** for MB photodegradation under visible light irradiation.

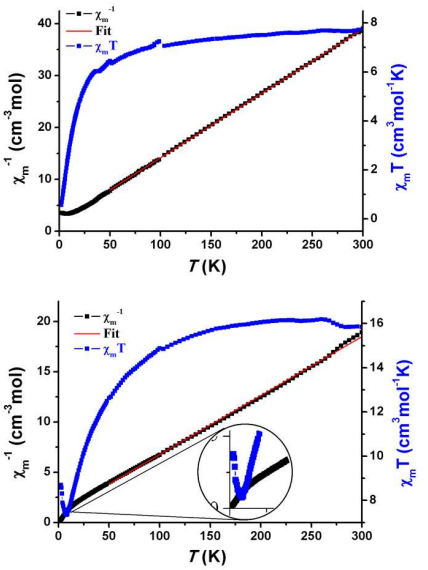

Fig. 6 Plots of χ_m and χ_mT versus temperature for **1** (up) and **5** (down).

state. Moreover, magnetism performance test is considered to be a good method to detect single electron coupling.[18] The magnetic properties of **1** and **5** in the form of χ_mT and χ_m versus T (χ_m being the molar magnetic susceptibility) plots are shown in Fig. 6. For complex **5**, the Co^{II} located in the octahedral environment is in a high spin state $(t_{2g})^5(e_g)^2$. The large value of χ_mT at 300 K is 15.78 cm^3 mol^{-1} K, suggests strong spin-orbit coupling interaction.[19] The χ_mT value rises abruptly at 9 K (Fig. 6 (down) inset), which is probably because of the ferrimagnetic behavior or a spin-canting response that evolves into long-range ordering.[20] The strong coupling interaction between single electrons may have the high activity to make it easier for d-d transition. However, for complex **1**, the Mn^{II} located in the octahedral environment is in a high spin state $(t_{2g})^3(e_g)^2$, and the half-full electronic state of **1**, can make valence electronics hard to be excited from VB to CB. Since the system is lack of excited electronics, photocatalytic reaction could not be performed. At the same time, the magnetic orbitals are composed of $d_{x^2-y^2}$ and d_{z^2}, and considerable contribution of the μ^2-O bridges is responsible for the overlap between d_{z^2} orbitals, which consequently induces antiferromagnetic interactions.[21] Obviously, the two complexes have exerted different magnetic behaviour of electrostatic interactions and the electron deficiency, which is corresponding to chemical environment of different center metals. This difference can lead to the disparate impact of photocatalytic behaviour.

The UV/Vis absorption spectrum can reflect the electron transition to some extent. The solid state absorption spectra of **1** and **5** at room temperature were investigated. As shown in Fig. S10, complexes **1** and **5** display similar absorption wavelength in ultraviolet region, which may be attributed to similar coordination configurations. However, in the visible light region (450-570 nm), complexes **1** and **5** show different maximum absorption peak. It may be due to the different metal ions that affect d-d transition energy. In order to study light absorption in detail, green light (535 nm) and blue light (450 nm) were selected as model photosource to evaluate the efficiency of photocatalysts, respectively. For **1**, it always acts an inhibitor regardless of which wavelength. It is possible to blame the mismatching between d-d transition energy and absorption of visible light, and the fewer photon absorbed could not provide appropriate energy to excite the electrons from the VB to the CB. Interestingly, **5** shows two different catalytic performance: reaction rate under green light is faster than that under blue light, which means the energy of green light are more suitable for exciting electrons. In addition, The band gaps (E_g) were defined as the intersection point between the energy axis and the line extrapolated from the linear portion of the adsorption edge in a plot of Kubelka-Munk function *F* versus energy *E*.[22] Kubelka-Munk function ($F=(1-R)^2/2R$) was transformed from the recorded diffuse reflectance data, where R is the reflectance of an infinitely thick layer at given wavelength. The *F* vs. *E* plots are revealed in Fig. S11. The E_g values evaluated from the steep absorption edge are 1.46 eV for **1** and 1.86 eV for **5**, which manifests that complexes **1** and **5** are underlying semiconductive materials.[23] The band gaps in **1** and **5** are similar, while the photocatalytic performances are quite opposite due to the influence of different chemical environment of center metals. Although the band gap of **1** is narrow, the occurrence of reactions was forbided. The possible explanation is that visible light cannot provide proper energy for the electrons in the valence band of complex **1** to be excited and Mn^{II} may combine with $\cdot O^{2-}$ and retard the formation of ·OH. Since the system is lack of ·OH, **1** shows inhibition to photocatalytic reaction.

In a word, the difference of photocatalytic performance between **1** and **5** are attributed to three reasons: (i) the strong spin-orbit coupling interaction of complex **5** shows that electrons are easily excited from the VB to the CB by electrostatic interactions, and the half-full electronic state of **1** make valence electronics hard to be excited. (ii) In complex **5**, the absorption of visible light may provide proper energy to excite electrons, while it has not been found in **1**. (iii) Mn^{II} may play an important role in inhibiting the photodegradation by retarding the formation of the hydroxyl radicals.

Conclusions

In conclusion, we have successfully synthesized and characterized a series of isostructural 2D coordination polymers $\{[Mn_3(L)_2(H_2O)_6]\cdot H_2O\}_n$ (**1**), intermediate M-M' (**2**-**4**) and $\{[Co_3(L)_2(H_2O)_6]\cdot H_2O\}_n$ (**5**). The photocatalytic properties of **1**-**5** have been examined, which show that **5** is photocatalytically active for degrading organic dyes under visible light lamp irradiation, while **1** can inhibit the photodegradation. When Mn ions are gradually replaced by Co ions in the complexes photocatalytic properties of **1**-**5** turn from inhibition to promotion, which is a controllable regulation of photocatalytic properties via changing metal ions. Currently, the following work will focus on preparing other new cluster-based coordination complexes with better photocatalytic activities for the degradation of organic dyes.

Acknowledgements

This work was financially supported by the National Natural Science Foundation (No. 21371155) and Research Fund for the Doctoral Program of Higher Education of China (20124101110002).

Notes and references

1 (a) L. L. Wen, F. Wang, J. Feng, K. L. Lv, C. G. Wang and D. F. Li, *Cryst. Growth Des.*, 2009, **9**, 3581; (b) J. Lv, J. X. Lin, X. L. Zhao and R. Cao, *Chem. Commun.*, 2012, **48**, 669; (c) P. P. Zhang, J. Peng, H. J. Pang, J. Q. Sha, M. Zhu, D. D. Wang, M. G. Liu and Z. M. Su, *Cryst. Growth Des.*, 2011, **11**, 2736.

2 (a) A. K. Paul, G. Madras and S. Natarajan, *Phys. Chem. Chem. Phys.*, 2009, **11**, 11285; (b) X. Zhuang, Y. Wan, C. Feng, Y. Shen and D. Zhao, *Chem. Mater.*, 2009, **21**, 706; (c) Y. Yan, M. Zhang, K. Gong, L. Su, Z. Guo and L. Mao, *Chem. Mater.*, 2005, **17**, 3457; (d) M. L. Ma, J. H. Qin, C. Ji, H. Xu, R. Wang, B. J. Li, S. Q. Zang, H. W. Hou, and S. R. Batten, *J. Mater. Chem. C*, 2014, **2**, 1085.

3 (a) W. S. W. Ngah and M. A. K. M. Hanafiah, *Bioresour. Technol*., 2008, **99**, 3935; (b) Y. Lee, S. G. Zimmermann, A. T. Kieu and U. V. Gunten, *Environ. Sci. Technol*., 2009, **43**, 3831; (c) J. Sarasa, M. P. Roche, M. P. Ormad, E. Gimeno, A. Puig and J. L. Ovelleiro, *Water Res.*, 1998, **32**, 2721.

4 (a) O. Legrini, E. Oliveros and A. M. Braun, *Chem. Rev.*, 1993, **93**, 671; (b) A. Mills, R. H. Davies and D. Worsley, *Chem. Soc. Rev*., 1993, **22**, 417; (c) J. Tang, Y. Liu, H. Li, Z. Tan and D. Li, *Chem. Commun*., 2013, **49**, 5498; (d) P. Mahata, G. Madras and S. J. Natarajan, *Phys. Chem. B*, 2006, **110**, 13759; (e) K. Rajeshwar, N. R.Tacconi and C. R. Chenth amarakshan, *Chem. Mater*., 2001, **13**, 2765; (f) X. L. Wang, J. Luan, F. F. Sui, H. Y. Lin, G. C. Liu and C. Xu, *Cryst. Growth Des*., 2013, **13**, 3561.

5 (a) Lin, H.; Maggard, P. A. *Inorg. Chem.*, 2008, **47**, 8044; (b) O. Legrini, E. Oliveros and A. M. Braunm, *Chem. Rev.*, 1993, **93**, 671; (c) A. Mills, R. H. Davies and D. Worsley, *Chem. Soc. Rev.*,1993, **22**, 417; (d) B. Liu, Z. T. Yu, J. Yang, H. Wu, Y. Y. Liu and J. F. Ma, *Inorg. Chem*., 2011, **50**, 8967; (e) H. X. Li, X. Y. Zhang, Y. N. Huo and J. Zhu, *Environ. Sci. Technol*., 2007, **41**, 4410; (f) Y. Z. Fan, R. M. Liu, W. Du, Q. Y. Lu, H Pang and F. Gao, *J. Mater. Chem.*, 2012 ,**22**, 12609.

6 (a) M. N. Chong, B. Jin and C. W. K. Chow, *Water Res*., 2010, **44**, 2997, (b) J. R. Li, Y. Tao, Q. Yu, X. H. Bu, H. Sakamoto and S. Kitagawa, *Chem. Eur. J*., 2008, **14**, 2771. (c) Y. Qiu, H. Deng, S. Yang, J. Mou, C. Daiguebonne, N. Kerbellec, O. Guillou and S. R. Batten, *Inorg. Chem*., 2009, **48**, 4158; (d) Q. G. Zhai, C. Z. Lu, X. Y. Wu and S. R. Batten, *Cryst. Growth Des.*, 2007, **7**, 2332.

7 (a) E. Piera, M. I. Tejedor, M. E. Zorn and M. A. Anderson, *Appl. Catal. B*, 2003, **46**, 671; (b) L. Liu, D. Q. Wu, B. Zhao, X. Han, H. W. Hou, *Dalton Trans*., 2015, **44**,1406; (c) Y. Q. Chen, S. J. Liu, Y.W. Li, G. R. Li, K. H. He, Y. K. Qu, T. L. Hu and X. H. Bu, *Cryst. Growth Des*., 2012, **12**, 5426,(d) Y. Q. Chen, G. R. Li, Y. K. Qu, Y. H. Zhang, K. H. He, Q. Gao and X. H. Bu, *Cryst. Growth Des*., 2013, **13**, 901; (e) J. Zhao, W. W. Dong, Y. P. Wu, Y. N. Wang, C. Wang, D. H. Li and Q. C. Zhang, *J. Mater. Chem. A*, 2015, **3**, 6962.

8 F. Fresno, R. Portel, S. Suarez and J. M. Coronado, *J. Mater. Chem. A*, 2014, **2**, 2863; (b) L. L. Wen, L. Zhou, B. Q. Zhang, X. Q Meng, H. Qu and D. F. Li, *J. Mater. Chem.*, 2012, **22**, 22603.

9 (a) Y. Hu, F. Luo and F. F. Dong, *Chem. Commun.*, 2011, **47**, 761; (b) W. Q. Kan, B. Liu, J. Yang, Y. Y. Liu and J. F. Ma, *Cryst. Growth Des.*, 2012, **12**, 2288; (c) H. Fu, Y. G. Li, Y. Lu, W. L. Chen, Q. Wu, J. X. Meng, X. L. Wang, Z. M. Zhang and E. B. Wang, *Cryst. Growth Des*., 2011, **11**, 458; (d) Q. Wu, W. L. Chen, D. Liu, C. Liang, Y. G. Li, S. W. Lin and E. Wang, *Dalton Trans*., 2011, **40**, 56.

10 (a) M. Q. Hu and Y. M. Xu, *Chemosphere.*, 2004, **54**, 431; (b) K. L. Lv and Y. M. Xu, J. *Phys. Chem. B*, 2006, **110**, 6204; (c) L. L. Wen, J. B. Zhao, K. L. Lv, Y. H. Wu, K. J. Deng, X. K. Leng and D. F. Li, *Cryst. Growth Des.*, 2012, **12**, 1603.

11 T. Wen, D. X. Zhang, J. Liu, R. Lin and J. Zhang, *Chem. Commun*., 2013, **49**, 5660; (b) L. Liu, J. Ding, C. Huang, M. Li and H. W. Hou, *Cryst. Growth Des.*, 2014, **14**, 3035.

12 (a) M. Dai, X. R. Su, X. Wang, B. Wu, Z. G. Ren, X. Zhou, and J. P. Lang, *Cryst. Growth Des.*, 2014, **14**, 240; (b) Y. Gong, P. G. Jiang, Y. X. Wang, T. Wu and J. H. Lin, *Dalton Trans.*, 2013, **42**, 7196; (c) H. Yang, X. W. He, F. Wang, Y. Kang and J. Zhang, *J. Mater. Chem*., 2012, **22**, 21849.

13 (a) Sheldrick, G. M. SHELXS-97: Program for the Solution of Crystal Structure; University of Göttingen: Göttingen, Germany, 1997; (b) Sheldrick, G. M. SHELXL-97, Program for the Crystal Structure Refinement; University of Göttingen: Göttingen, Germany, 1997.

14 (a) L Qin, Z. J. Wang, T Wang, H. G. Zheng and J. X. Chen, *Dalton Trans*., 2014, **43**, 12528; (b) R. X. Yao, X. Xu and X. M. Zhang, *Chem. Mater*., 2012, **24**, 303; (c) J. H. Cui, Y. Z. Li, Z. J. Guo, and H. G. Zheng, *Cryst. Growth Des.*, 2012, **12**, 3610;(d) M. Du, X. G. Wang, Z. H. Zhang, L. F. Tang and X. J. Zhao, *CrystEngComm*., 2006, **8**, 788; (e) D. Cheng, M. A. Khan, and R. P. Houser, *Cryst. Growth Des.*, 2004, **4**, 599; (f) D. Cheng, M. A. Khan and R. P. Houser, *J. Chem. Soc., Dalton Trans.*, 2002, 4555.

15 M Du, Z. H. Zhang, L. F. Tang, X. G. Wang, X. J. Zhao and S. R. Batten, *Chem. Eur. J.* 2007, **13**, 2578.

16 (a) F. Wang; Z. S. Liu, H. Yang, Y. X. Tan and J. Zhang, *Angew. Chem. Int. Ed.*, 2011, **50**, 450; (b) C. N. Lv, M. M. Chen, W. H. Zhang, D. X. Li, M. Dai and J. P. Lang, *CrystEngComm.*, 2015, **17**, 1935.

17 (a) G. H. Cui, C. H. He, C. H. Jiao, J. C. Geng and V. A. Blatov, *CrystEngComm*., 2012, **14**, 4210; (b) B. Ahmed, E. Limem, A. A. Wahab and B. Nasr, Ind. Eng. *Chem. Res.*, 2011, **50**, 6673; (c) A. Corma, H. Garcia and F. X. L. Xamena, *Chem. Rev.*, 2010, **110**, 4606.

18 (a) W. Meng, H. J. Li, Z. Q. Xu, S. S. Du, Y. X. Li, Y. Y. Zhu, Y. Han and H. W. Hou, *Chem. Eur. J.*, 2014, **20**, 2945; (b) M. X. Zheng, X. J. Gao, C. L. Zhang, L. Qin and H. G. Zheng, *Dalton Trans*., 2015, **44**, 4751; (c) J. P. Zhao, Q. Yang,Z. Y. Liu, R. Zhao, B. W. Hu, M. Du, Z. Chang and X. H. Bu, *Chem. Commun*., 2012, **48**, 6568.

19 (a) C. Y. Sun, X. J. Zheng, S. Gao, L. C. Li and L. P. Jin, *Eur. J. Inorg. Chem.*, 2005, **20**, 4150; (b) D. S. Li, J. Zhao, Y. P. Wu, B. Liu, L. Bai, K. Zou, and M. Du, *Inorg. Chem.*, 2013, **52**, 8091; (c) M. H. Zeng, Y. L. Zhou, M. C. Wu, H. L. Sun and M. Du, *Inorg. Chem.*, 2010, **49**, 6436.

20 L. Liu, X. F. Lv, L. Zhang, L. A. Guo and H. W. Hou, *CrystEngComm.,* 2014, **16**, 8736.

21 (a) J. M. Rueff, N. Mascicchi, P. Rabu, A. Sironi and A. Skoulios, *Eur. J. Inorg. Chem.*, 2001, 2843; (b) M. Nakano and H. Oshio, *Chem. Soc. Rev.*, 2011, **40**, 3239; (c) L. F. Ma, M. L. Han, J. H. Qin, L. Y. Wang, and M. Du, *Inorg. Chem*., 2012, **51**, 9431.

22 W. Q. Kan, B. Liu, J. Yang, Y. Y. Liu and J. F. Ma, *Cryst Growth Des.*, 2012, **12**, 2288; (b) Y. Gong, Z. Hao, J. L. Sun, H. F. Shi, P. G. Jiang, J. H. Lin, *Dalton Trans.*, 2013, **42**, 13241; (c) L. Zhang, Y. Wei, C. Wang, H. Guo, P. J. Wang, *Solid State Chem*., 2004, **177**, 3433; (d) M. D. Allendorf, C. A. Bauer, R. K. Bhaktaa, R. J. T. Houka, *Chem. Soc. Rev.*, 2009, **38**, 1330; (e) M. R. Santacruz, A. E. Sepulveda, E. Serrano, E. Lalinde, J. R. Berenguer and J. G. Martınez *J. Mater. Chem. C*, 2014, **2**, 9497.

23 (a) J. Guo, J. F. Ma, B. Liu, W. Q. Kan and J. Yang, *Cryst. Growth Des*., 2011, **11**, 3609; (b) H. S. Liu, Y. Lan and S. L. Li, *Cryst. Growth Des*., 2010, **10**, 5221. (c) H. X. Qi, J. F. Wang, Z. G. Ren, J. J. Ning and J. P. Lang, *Dalton Trans.*, 2015, **44**, 5662; (d) H. T. Cao, G. G. Shan, X. M. Wen, H. Z. Sun, Z. M. Su, R. L. Zhong, W. F. Xie, P. Li and D. X. Zhu, *J. Mater. Chem. C*, 2013, **1**, 7371; (e) H. B. Zhang, X. C. Shan, L. J. Zhou, P. Lin, R. F. Li, E. Ma, X. G. Guo and S. W. Du, *J. Mater. Chem. C*, 2013, **1**, 888.

The Effect of Metal Ions on Photocatalytic Performance Based on Isostructural Framework

Zhichao Shao, Chao Huang, Xiao Han, Huarui Wang, Angran Li, Yanbing Han, Kai Li*, Hongwei Hou* and Yaoting Fan

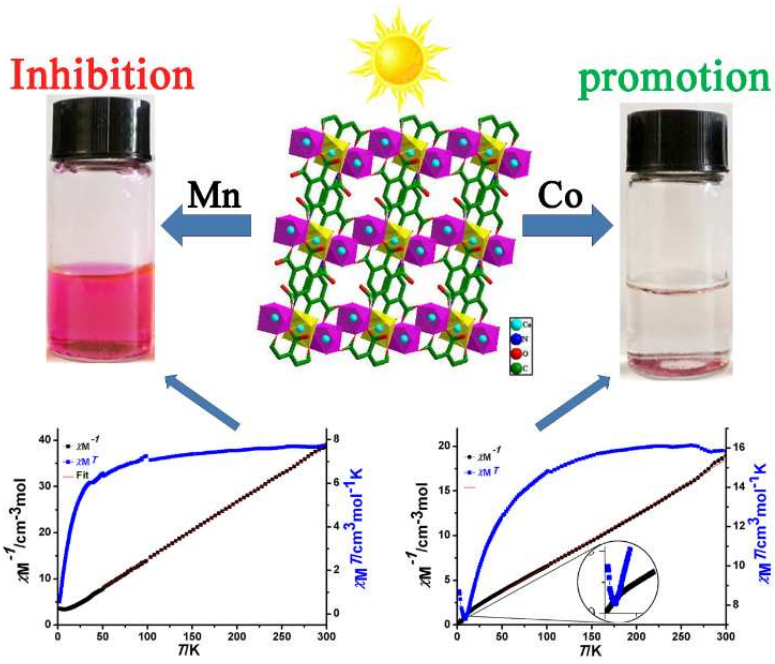

The different center metal ions in CPs have a variety of electronic configurations, which can produce a great impact on the photocatalytic properties.